RESEARCH ARTICLE

Visuo-motor transformations involved in the escape response to looming stimuli in the crab *Neohelice* (=*Chasmagnathus*) *granulata*

Damián Oliva[1,2] and Daniel Tomsic[2,*]

[1]Departamento de Ciencia y Tecnología, Universidad Nacional de Quilmes, Roque Saenz Peña, Bernal (1876), Provincia Buenos Aires, Argentina and [2]Laboratorio de Neurobiología de la Memoria, Departamento Fisiología, Biología Molecular y Celular, Facultad de Ciencias Exactas y Naturales, Universidad de Buenos Aires, IFIBYNE-CONICET, Pabellón 2 Ciudad Universitaria (1428), Ciudad de Buenos Aires, Argentina

*Author for correspondence (tomsic@fbmc.fcen.uba.ar)

SUMMARY

Escape responses to directly approaching predators represent one instance of an animal's ability to avoid collision. Usually, such responses can be easily evoked in the laboratory using two-dimensional computer simulations of approaching objects, known as looming stimuli. Therefore, escape behaviors are considered useful models for the study of computations performed by the brain to efficiently transform visual information into organized motor patterns. The escape response of the crab *Neohelice* (previously *Chasmagnathus*) *granulata* offers an opportunity to investigate the processing of looming stimuli and its transformation into complex motor patterns. Here we studied the escape performance of this crab to a variety of different looming stimuli. The response always consisted of a vigorous run away from the stimulus. However, the moment at which it was initiated, as well as the developed speed, closely matched the expansion dynamics of each particular stimulus. Thus, we analyzed the response events as a function of several variables that could theoretically be used by the crab (angular size, angular velocity, etc.). Our main findings were that: (1) the decision to initiate the escape run is made when the stimulus angular size increases by 7 deg; (2) the escape run is not a ballistic kind of response, as its speed is adjusted concurrently with changes in the optical stimulus variables; and (3) the speed of the escape run can be faithfully described by a phenomenological input–output relationship based on the stimulus angular increment and the angular velocity of the stimulus.

Key words: visual behavior, escape response, looming detection, Crustacea.

Received 30 January 2012; Accepted 7 June 2012

INTRODUCTION

Collision avoidance behaviors are of particular interest in view of their biological importance. In effect, most visual animals are highly efficient in detecting and avoiding collisions, which may occur either by encounters with obstacles while they move, or by moving objects that directly approach them. Natural instances of objects approaching on a collision course are the sudden attacks of predators. The maneuvers executed to evade predatory assaults are paramount behaviors that must be controlled by rather straightforward neural circuits to generate quick and reliable avoidance responses. To be effective, those responses need to be executed in a timely manner, which implies that the approaching object must be monitored in real time for the animal to decide whether, when and how to generate an escape response. Approaching objects can be effectively simulated using two-dimensional projections on a computer screen, called looming stimuli. Neurophysiological investigations in species as diverse as locusts, fish and pigeons have shown striking similarities regarding the sensory processing of looming stimuli (Rind and Simmons, 1999; Fotowat and Gabbiani, 2011; Preuss et al., 2006; Sun and Frost, 1998). However, the differences between the motor systems used by these animals to perform escape responses are enormous, raising the question of whether common sensory-motor transformation rules are exploited in species with similar sensory processing stages. Because of this, in the concluding remarks of their recent review on collision avoidance behavior,

Fotowat and Gabbiani (Fotowat and Gabbiani, 2011) emphasized the need of comparative studies to draw general conclusions about the way in which brains process information and organize the motor outputs that allow animals to avoid collision. Unfortunately, the number of animal models that proved to be suitable for behavioral as well as neuronal analysis of responses to looming stimuli is still scarce.

In a previous paper, we introduced a new experimental model using the crab *Neohelice granulata*, which offers good opportunities for investigating the processes of looming detection, escape decision and motor control at both behavioral and neuronal levels (Oliva et al., 2007). Briefly, in its natural environment, this crab is predated by gulls and, consequently, reacts to the image of an approaching object by running away in the opposite direction. The escape response can be readily elicited in the laboratory using looming stimuli and accurately measured with a treadmill-like device. In addition, the response of identified neurons from the lobula (third optic neuropile of arthropods), some of which responded to looming stimuli in a way that parallels behavior, can be electrophysiologically recorded *in vivo* (Berón de Astrada and Tomsic, 2002; Medan et al., 2007; Oliva et al., 2007; Sztarker and Tomsic, 2008).

Avoidance responses to looming stimuli range from ballistic-like behaviors to more complex ones where the response is continually adjusted while being performed according to the observed changes in the approaching stimulus direction and speed. The first types of

responses, which can be described as single threshold response systems, are triggered when an optical variable of the image exceeds a certain value, after which the animal displays a stereotyped behavior. This type of response has been described in species such as crayfish (Glantz, 1974) and fish (Preuss et al., 2006). In other cases, the avoidance response is composed of distinctive preparatory stages, each one being triggered when an optical variable reaches a particular threshold. Examples of this multistage type of response can be found in flies (Borst and Bahde, 1988; Tammero and Dickinson, 2002; Card and Dickinson, 2008a; Card and Dickinson, 2008b), crabs (Hemmi and Pfeil, 2010) and locusts (e.g. Santer et al., 2005a; Santer et al., 2005b; Santer et al., 2006; Santer et al., 2008; Gray et al., 2001; Fotowat and Gabbiani, 2007; Fotowat et al., 2011). Finally, there are avoidance responses that are continuously adjusted to external changes, such as those occurring during unpredictable modifications of the trajectory or velocity of predatory attacks. These responses can be described as continually regulated systems. Behaviors guided by continually regulated systems have been mostly studied in the context of animal navigation (e.g. Srinivasan et al., 2000; Fry et al., 2009), but not as much in the context of predator avoidance (Land and Layne, 1995).

Our previous characterization of the response to a single looming stimulus in the crab (Oliva et al., 2007) has provided some indications that this behavior would consist of a threshold-type decision for initiating the escape run, followed by a visually regulated mechanism for continually controlling the velocity of the escape run. Here, we evaluated this hypothesis by analyzing the responses of crabs to a wide variety of looming stimuli that differed in size and approaching velocity. The analysis led us to the identification of the optical stimulus' variables that the animal most likely takes into account to perform the behavioral response. Moreover, we propose a phenomenological input–output relationship based only on these variables that allow us to predict the behavioral performance in response to the different dynamics of approaching objects.

MATERIALS AND METHODS
Animals
Animals were adult male *Neohelice* (previously *Chasmagnathus*) *granulata* (Dana 1851) crabs 2.7–3.0 cm across the carapace, weighing approximately 17 g, collected in the rías (narrow coastal inlets) of San Clemente del Tuyú, Argentina, and transported to the laboratory, where they were lodged in plastic tanks (35×48×27 cm) filled to 2 cm depth with diluted seawater at a density of 20 crabs per tank. Water used in tanks and other containers during the experiments was prepared using hw-Marinex (Winex, Hamburg, Germany), salinity 10–14‰, pH 7.4–7.6, and maintained within a temperature range of 22–24°C. The holding and experimental rooms were maintained on a 12 h:12 h light:dark cycle (lights on 07:00 to 19:00 h) and the experiments were run between 08:00 and 19:00 h. Experiments were performed within the first 2 weeks after the animals arrived. Crabs were fed rabbit pellets (Nutrients, Buenos Aires, Argentina) every 3 days and after feeding the water was changed. Following experiments, animals were returned to the field and released in a location 30 km from the capture area.

Visual stimuli and behavioral recording setup
Computer-generated visual stimuli were projected either simultaneously or alternatively on five flat-screen monitors (Phillips 107T; horizontal and vertical screen dimensions were 32 and 24 cm, respectively, refresh rate 60 Hz), located 20 cm to the front, back, both sides and above of the animal (Oliva et al., 2007).

The monitors were covered with anti-glare screens to reduce reflections between them. All visual stimuli were generated with a PC using commercial software (Presentation 5.3, Neurobehavioral Systems, Albany, CA, USA). Because we were particularly interested in investigating the response initiation and running speed, the experiments were performed with stimuli presented only on the monitor located at the animal's right to keep the image of the approaching stimulus at a fixed position on the lateral pole as the crab runs sideways (Land and Layne, 1995). We have previously shown that the initial response time is the same for stimuli approaching frontally or laterally (Oliva et al., 2007). However, when the stimulus is approaching frontally, the escape response includes an initial rotational component that allows the animal to run sideways. This rotation maneuver makes the analysis of the run velocity more difficult, a complication that we wished to avoid at this stage. Besides, stimuli appearing from the lateral pole are seen by the animal monocularly, which made our results comparable with those obtained in locusts and pigeons (reviewed in Rind and Simmons, 1999; Fotowat and Gabbiani, 2011).

The effectiveness of 2-D computer images to elicit the crab's escape response has been already shown (Oliva et al., 2007). Moreover, in recent experiments we found no differences between the escape response elicited by a black sheet of cardboard approaching the animal and the computer simulation of an object of the same size and speed of approach (Oliva, 2010).

The locomotor activity of the crab was investigated in a walking simulator device that has been described in detail elsewhere (Oliva et al., 2007). Briefly, it consisted of a floating Styrofoam ball that could be freely rotated by the locomotor activity of an animal, attached in a standing position to a weightless rod through a piece of rubber glued to its dorsal carapace. The rod was introduced inside a metal guide, positioned vertically above the ball, where it could slide up and down with little friction (Fig. 1A). This allowed the animal to feel its own weight and thus adopt its natural posture while performing on the ball. The rod and guide both had square sections, which prevented rotational movements and thus assured that the animal always saw the stimulus with the same side of the eye (the lateral pole in this study). The Styrofoam ball (16 cm in diameter) floated within a bowl-shaped container partially filled with water. Horizontal displacements of the ball were prevented by four set points provided by two optical mice and two flexible sheets located at right angles from each other. The rotation of the ball was recorded by the two mice, with their optical reading systems protected by transparent acetate sheets, which also guaranteed the smooth movement of the ball. Locomotion signals were acquired using the recording facilities of the same commercial software that generated the visual stimuli. Mice data were taken at each frame update (16.7 ms), which assured an accurate correspondence between the recorded response times and the stimulus features (size, border speed, etc.). Two Presentation programs were run on two separate PCs. The PC that generated the visual stimuli (PC1) was used to record one of the mice and to trigger the recording by the second mouse in the second PC (PC2). Hence, the program that generated the visual stimulus synchronized the recording of the two mice just before stimulus onset. The data from mice 1 and 2 during a trial generated two Presentation files, which contained a list of times associated with each data record and frame update. Further detail on data recording and analysis can be found in Oliva et al. (Oliva et al., 2007). Behavior was also monitored by visually observing the animal online through a video camera.
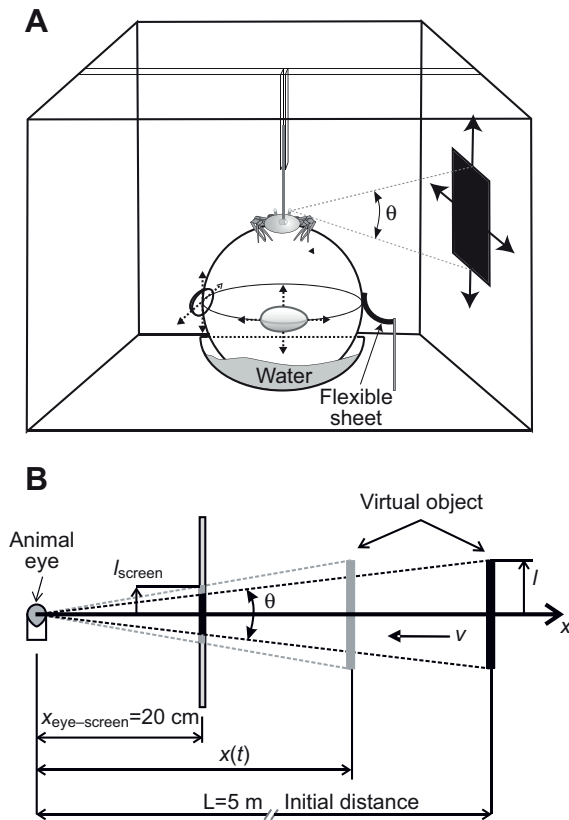
A

B

Fig. 1. (A) Measurement of the escape response. Locomotor activity was studied in a walking simulator device that consisted of a Styrofoam ball that could be freely rotated by the animal. The crab was held in position by a weightless rod attached to its carapace that could slide up and down within a guide located above the animal. Both the rod and the guide sleeve had square cross-sections, which prevented the animal from rotating around its yaw axis. Locomotion was assessed by recording the rotations of the ball with two computer mice as described elsewhere (Oliva et al., 2007). The ball and the crab were surrounded by five screen monitors, each located 20 cm from the animal. (B) Simulation of an object's approach at constant speed. The right eye of the crab was stimulated from the right side by presenting squares of half-size l approaching at a constant speed v towards the center of the eye, at 90 deg relative to the animal's body axis. The figure shows the virtual object at two different times during the simulated approach. $x(t)$ is the position of the object in a reference system centered at the crab's right eye, $\theta(t)$ is the total subtended angle for the object at the crab's eye, and l_{screen} is the half-size of the square drawn on the monitor screen.

Kinematics of object approach

The stimuli used were simulated dark squares of various sizes approaching with constant speeds on a direct collision course to the animal (Fig. 1B). Let l denote the object half-size. The distance between the animal eye and object at time t is $x(t)$ and the object subtends an angle $\theta(t)$ on the eye. Thus, we can write:

$$\tan[\theta(t)/2] = l/x(t). \tag{1}$$

With the chosen coordinate system and time definitions, we have $x(t) \geq 0$, $t \geq 0$. Objects were simulated to start their approach from a distance of $L=5$ m. The position of the object is defined by:

$$x(t) = L - vt, \tag{2}$$

where v is the absolute value of the approach speed.

The square drawn on the monitor screen (Fig. 1B) has a half-size $l_{\text{screen}}(t)$ and depends on the distance from the monitor to the eye of the animal, $x_{\text{eye–screen}}$, as follows:

$$\tan(\theta/2) = \frac{l_{\text{screen}}}{x_{\text{eye–screen}}} = \frac{l}{x(t)}. \tag{3}$$

Replacing $x(t)$ with $L-vt$ from Eqn 2, and solving for $l_{\text{screen}}(t)$, we get:

$$l_{\text{screen}}(t) = \frac{x_{\text{eye–screen}}l}{x(t)} = \frac{x_{\text{eye–screen}}l}{L - vt}. \tag{4}$$

Eqn 4 describes a half-size square drawn on the screen monitor as a function of time. Because of the limits imposed by the screen's size and distance to the animal's eye, maximum stimulus expansion was $\theta=60$ deg.

In the literature regarding looming detection the dynamic of a stimulus expansion is usually characterized by the relationship l/v (Gabbiani et al., 1999). By replacing $x(t)$ from Eqn 2 in Eqn 3, we get:

$$\tan(\theta/2) = \frac{l}{L - vt} = \frac{1}{L/l - vt/l} = \frac{1}{1/\tan(\theta_0/2) - t/(l/v)}. \tag{5}$$

From Eqn 5 it can be observed that in the present study each stimulus is characterized by two values, one of l/v and one of θ_0.

Stimuli used

We used a total of eight stimuli (Table 1). For stimuli 1–4 we maintained the approach speed $v=142.5\,\text{cm s}^{-1}$ and varied the size l from 8.5 to 64 cm. The subtended angle of the smallest stimulus at the initial distance was 1.8 deg, which is well above the sampling resolution of the crab's eye. In fact, in the lateral part of the eye the resolution reaches values between 0.83 and 1.2 cycles deg^{-1}, corresponding to interommatidial angles between 0.6 and 0.4 deg, respectively (Berón de Astrada et al., 2012). Thus, animals would not have optical limitations to detect differences between initial sizes of the smaller stimuli used here. For stimuli 5–8 we kept $l=17$ cm and varied v from 35.5 to 286 cm s^{-1}. These speeds were used to simulate predators that approach the animal faster than its ability to run away (*Neohelice*'s highest escape speed is 35 cm s^{-1}). Moreover, this minimized the compensation of the stimulus growth by the animal's speed developed while attempting to get away. Stimuli 2 and 7 had the same size and expansion dynamics; hence they were indistinguishable by the animal from each other. The similarities in the results obtained with these two stimuli served as an internal control for each experimental series.

Conditions of stimulation

In Oliva et al. (Oliva et al., 2007) we described some important features of the escape response and optimal stimulation parameters such as interval between trials, the direction of approach and object contrast against the background. Based on those results, we began stimulation after the animal had remained visually undisturbed for 10 min inside the setup. In all trials, the stimulus remained stationary for 30 s at its initial position before starting to increase in size. The inter-trial interval was set to 3 min to reduce habituation and fatigue effects [fig. 5 in Oliva et al. (Oliva et al., 2007)]. Stimuli were applied only from the right to reduce variability [fig. 6 in Oliva et al. (Oliva et al., 2007)]. We used black squares expanding on a white background [fig. 10 in Oliva et al. (Oliva et al., 2007)]. Radiance on the monitor screen was 4 mW m^{-2} (black square) and 240 mW m^{-2} (background). The eight stimuli in Table 1 were applied to each animal in a random order, and only once.

Table 1. Parameters of looming stimuli (see Fig. 1B)

Stimulus number	l (cm)	V (cm s^{-1})	l/v (ms)	L (m)	T (s)	θ_0 (deg)
1	8.5	142.5	60	5	3.5	1.8
2	17	142.5	120	5	3.5	3.9
3	32	142.5	225	5	3.5	7.3
4	64	142.5	450	5	3.5	14.5
5	17	35.5	479	5	14	3.9
6	17	71.5	238	5	7	3.9
7	17	142.5	120	5	3.5	3.9
8	17	286	60	5	1.75	3.9

l is the half-size of the object, v is the approach speed, L is the initial distance, T is the travelling time of the simulated approaching object and θ_0 is the initial angular size of the object.

Animal and response selection

All the animals challenged with the looming stimulus in the present study consistently displayed escape responses. In some trials animals were walking when the expansion started. Results of ongoing experiments suggest that this does not affect response initiation times. However, to simplify the analysis, we used only those trials where the animals were motionless before the beginning of the expansion (>85% of trials). Additionally, we excluded those responses in which the traveled distance during the expansion was below 10% of the mean response for that stimulus (this corresponded to less than 5% of responses).

Criteria for the beginning of the escape response

We defined the beginning of the escape run as the moment in which the recording trace showed the animal's first movement after the expansion of the image had initiated. This first stepping movement is easily detected and is characteristically followed by a progressive increase in the animal's speed [see fig. 4 in Oliva et al. (Oliva et al., 2007)]. The time of escape t_{esc} then corresponded with the time interval between the beginning of the stimulus expansion (t=0) and the moment when the animal initiated the escape. Each trace was examined separately and t_{esc} was obtained for every trial in all the animals.

Data analysis

To estimate the animal's speed we convolved the instantaneous speed with a 100 ms square window and normalized the resulting waveform (Gabbiani et al., 1999). Least-squares regressions of the animal's speed with respect to stimulus optical variables described later in the Results were used to fit the input–output relationship between these variables and the escape speed. The Kruskal–Wallis test was used to compare the medians of samples across different stimuli. Unless otherwise stated, the P-values were derived from the Kruskal–Wallis test. When no significant differences were found, we report average values across treatments. To analyze the visuomotor delay we computed the Pearson correlation coefficient between different kinematic variables with the parameters l/v and θ_0 (Table 1) at a fixed processing delay δ before escape (Fotowat and Gabbiani, 2007). Data analysis procedures were written in MATLAB (The MathWorks, Natick, MA, USA). Further procedures are explained in the Results.

RESULTS

The aim of the present study was to identify which optical variable in a looming stimulus (e.g. angular size, angular velocity) is first used by the crab to decide to begin an escape run and regulate its speed. In other words, we expected to find a variable and a mathematical function that would allow us to predict the initiation and speed of the response to looming stimuli. This required the analysis of responses to different stimulus sizes and speeds of approach, thus exhibiting distinct expansion dynamics, and the search for the threshold value of an optical variable common to all stimuli at the time that a particular behavioral event occurred (e.g. when the escape response started or when the crab ran at a particular speed).

Fig. 2 shows the mean responses of a group of 20 crabs to the eight looming stimuli that were used in this study (Table 1). Because all stimuli approached from the same side, the responses were highly directional [fig. 6 in Oliva et al. (Oliva et al., 2007)]. The temporal course of the responses was as follows: animals were initially motionless and remained so even when the stimulus had begun its expansion, then suddenly they started running in the opposite direction to the stimulus (arrows in each trace mark the mean t_{esc}). Statistical differences between the mean t_{esc} of stimuli 1 and 2 (arrows below the pink and red traces in Fig. 2, respectively, P<0.05) indicate that animals were able to distinguish between the smaller stimulus sizes used in this study. After the initial movement, the animals gradually increased their speed as the object grew larger, as if they were 'tracking' the object over its approach until the expansion was completed, after which speed was suddenly reduced. For all stimuli, we found the same response stages previously described for a single stimulus (Oliva et al., 2007). Individual responses are shown in Fig. 3A and in figs 3 and 4 of Oliva et al. (Oliva et al., 2007).

Optical variables that may predict the onset of escape run

We assumed that crabs made the decision to initiate the escape from looming stimuli based on threshold criteria, i.e. the escape began after a certain optical variable had reached a particular value. The analysis therefore sought to identify a variable with a common value for all the stimuli at the moment the animal made the decision to escape. In our analyses we took into consideration several optical variables, Z_{1-6} (Table 2), that the crab could compute to decide the escape, some of which have been shown to be important in studies with different animal species (see Introduction). The following is a description of these variables. All of them are described at $t_{esc}-\delta$, where δ is the delay between the animal decision for escape and the actual behavioral measurement (see below).

Time elapsed since the beginning of the expansion

The animal begins the escape a fixed time after detecting the beginning of the expansion. We called this variable: $Z_1=t_{esc}-\delta$.

Time to collision

Some animals (e.g. pigeons) have neurons that are activated a fixed time before the collision occurs (Wang and Frost, 1992). Therefore, we measured the time to collision t_c, δ milliseconds before the escape, and named this variable: $Z_2=t_c(t_{esc}-\delta)$.
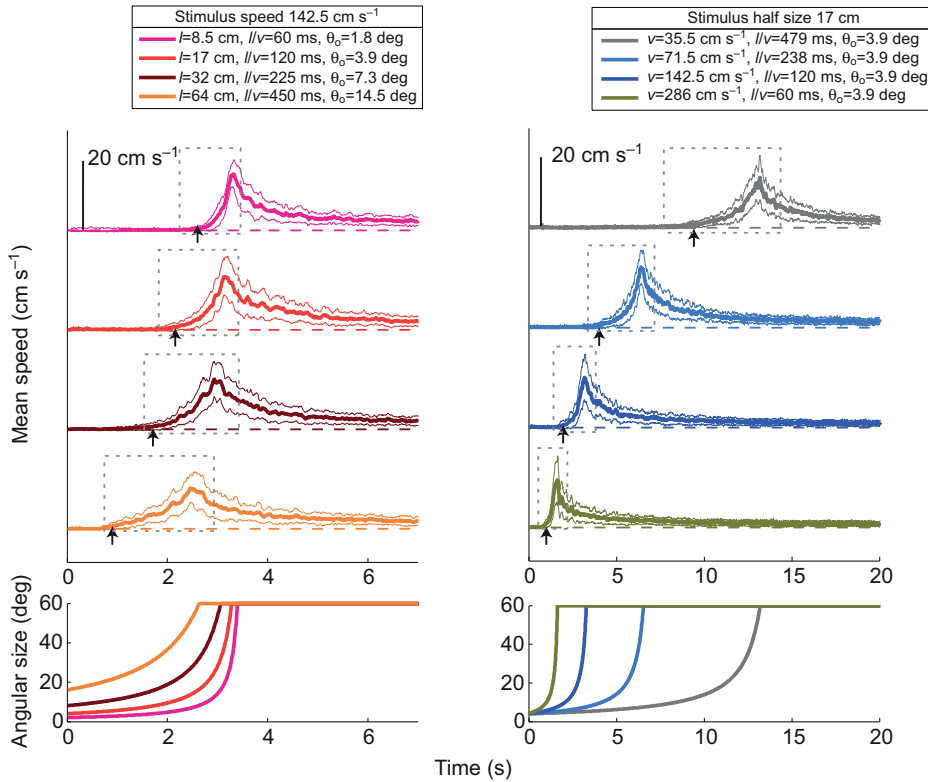
Fig. 2. Mean instantaneous speed of escape to different stimuli, identified by a color code. Thin lines represent the standard deviation of the mean. The left column corresponds to stimuli 1–4 in Table 1, which share the same speed but have different sizes. The right column corresponds to stimuli 5–8, which share the same size but have different speeds. Arrows below each trace mark mean escape initiation times (t_{esc}). Each animal received all the stimuli, one every 3 min, in random order (N=20 animals). Notice the matching between stimulus expansion dynamics and response performance throughout the stimuli. Dashed line rectangles enclose the portion of the response corresponding to the time of stimulus expansion (used later in Fig. 11). The bottom two panels show the expansion dynamics (angular size) for the eight stimuli listed in Table 1.

Angular size, angular velocity or angular acceleration

Some animals produce collision avoidance responses when the angular size of the stimulus has reached a threshold (Fotowat and Gabbiani, 2007). Angular velocity (Hemmi, 2005b) or angular acceleration are two other alternatives that might be taken into consideration. Therefore, we evaluated angular size $Z_3=\theta(t_{esc}-\delta)$, angular velocity $Z_4=\dot{\theta}(t_{esc}-\delta)$ and angular acceleration $Z_5=\ddot{\theta}(t_{esc}-\delta)$.

Angular increment

Finally, animals might consider the angular increment, which we named $Z_6=\Delta\theta(t_{esc}-\delta)=\theta(t_{esc}-\delta)-\theta(t=0)$. The crayfish defensive reflex occurs when the angular size of the approaching object increases by 8 deg (Glantz, 1974).

Time delay between the decision and the measurement of the escape

Once the decision to initiate the escape has been made, additional time is required for the behavior to occur, such as the time consumed in conveying the message downstream through the neural system and to the muscles, and to generate the forces necessary to move the legs and overcome the inertia of the recording device. Consequently, the optical variables must be analyzed at time $t_{esc}-\delta$, where δ is the delay between the moment the animal decided to escape and its associated motor response (see Fig. 3B). The magnitude of δ is then crucial for ascertaining the value attained by the optical parameters at the time of the escape decision. An error in the value of δ would render differential
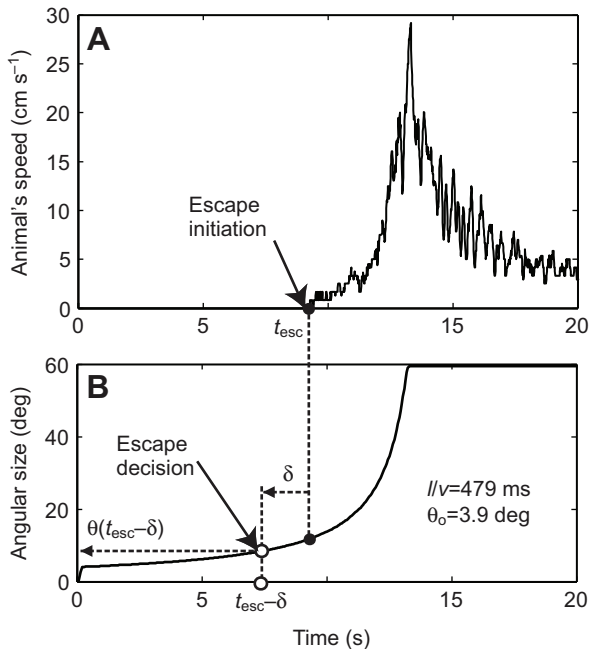

Fig. 3. Representation of the measurement of an optical variable when the animal decides to begin the escape run. (A) Speed of an individual response to a looming stimulus. (B) Angular size $\theta(t)$ of the stimulus as a function of time. The optical variable (in this case angular size θ) should be assessed at time $t_{esc}-\delta$, where δ is the delay between the moment at which the animal decides to escape and the associated measured response. The value of δ in the figure is drawn out of scale.

Table 2. Variables that animals could compute to decide to start an escape run

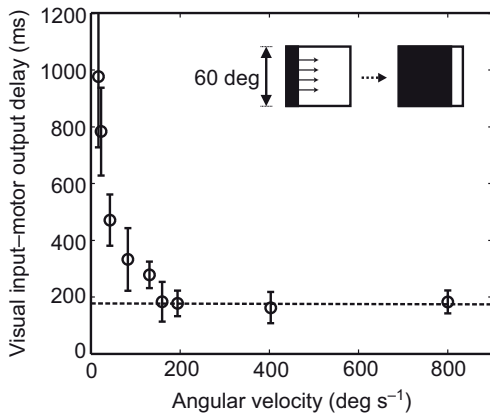| Variable	Notation	Description
Z_1	t_{esc}	Escape time
Z_2	t_c	Time to collision
Z_3	θ	Angular size
Z_4	$\dot{\theta}$	Angular velocity
Z_5	$\ddot{\theta}$	Angular acceleration
Z_6	$\Delta\theta$	Angular increment

Fig. 4. Estimation of the delay between the visual input and the motor output. The inset depicts the stimulus used for this experiment: a black edge of 60 deg height advancing on a white background with constant angular velocity. The graph shows the latency between the start of the stimulus movement and the measured response as a function of the stimulus angular velocity. The latency decreased with increasing stimulus speeds to a minimum asymptotic value of 170 ms. This value would correspond to the minimum time required to convey visual information downstream towards the motor system and move the walking device. A realistic estimate of δ, however, must also consider the time elapsed between the moment when the visual information reaches the retina and the moment when the decision is made (see further explanations in the Results).

errors in the values of the optical variable associated with the escape decision for the different looming stimuli. Thus, we were required to measure the magnitude of δ as precisely as possible. For this reason we performed an experiment where we challenged the animals with a visual stimulus that could be taken as a threat as soon as it appeared; the threat consisted of a black edge spanning 60 deg in elevation that progressed horizontally from one side to the other of the lateral monitor (see Fig. 4 inset). Unlike approaching objects, which usually begin subtending a small angular size that does not provoke an escape until expanding to some extent, a large visual stimulus moving fast enough would be interpreted as an immediate danger, thus instantly prompting an escape response. Therefore, the delay between the visual input and the motor output for this stimulus likely corresponds to the minimal latency obtained between the onset of stimulus motion and the onset of escape. Fig. 4 shows the latency of the escape response as a function of the angular velocity of the stimulus' tangential motion. The delay was ~1 s at low angular velocities (20 deg s^{-1}), but was reduced gradually to an asymptotic minimum value of 170 ms for angular velocities of 180 deg s^{-1} and beyond. From this experiment we concluded that the delay between visual input and behavioral measurement of the escape was 170±25 ms (mean±s.e.m.). The decision, however, cannot be thought to occur just as the visual stimulus reaches the retina, but rather at a deeper brain level. A substantial amount of evidence suggests that the decision to escape from visual stimuli may arise at the level of the giant neurons of the lobula (e.g. Tomsic et al., 2003; Sztarker and Tomsic, 2008; Sztarker and Tomsic, 2011), which present a response delay to visual stimuli of ~35 ms (Medan et al., 2007). This time has to be subtracted from the visual input to motor output delay calculated above in order to obtain a realistic estimation of the elapsed time between the decision-making process and the actual escape recording. Therefore, δ=170–35=135 ms.

What optical variable best predicts the onset of escape run?

All optical variables were measured at t_{esc}–δ in every trial for each animal. We then analyzed whether any of the variables Z_{1-6} attained a constant value for all the stimuli at the moment the animals decided to initiate their escape run. Fig. 5 shows the results. Of the six variables analyzed, angular increment was the only one whose value remained constant throughout the stimuli (P=0.6). None of the other variables met this criterion; they all presented significant differences among the stimuli (P<0.001). Therefore, we concluded that the escape is initiated when angular increment exceeds a mean (±s.e.m.) value of ~7±0.3 deg (dashed line in Fig. 5F).

The previous analysis was made with the δ value derived from experiments using a translating stimulus (Fig. 4). It could be argued that the effective delay used by the crab for approaching stimuli may not be the same as that used for translating stimuli, thus casting doubts on our conclusions. Therefore, we performed a different analysis to test whether angular increment or any other kinematic stimulus variable was equal to a constant threshold at a fixed delay before escape initiation. This analysis, used by Fotowat and Gabbiani (Fotowat and Gabbiani, 2007) to identify the optical variable best related to the locust takeoff time upon looming stimuli, allows us to determine the delay directly from the experimental data obtained with the looming stimuli. According to this analysis, a necessary condition for angular increment to be constant at a certain delay before escape initiation is that its correlation coefficient with l/v is zero at that delay. Therefore, we systematically computed the correlation coefficient between angular increment and l/v as a function of time before escape (Fig. 6, dark blue curve). In the case of angular increment, the correlation coefficient was zero around 140 ms before escape initiation time. This estimation of the delay was in close agreement with that obtained experimentally using translating stimuli (135 ms). Furthermore, the correlation analysis clearly shows that angular increment is the only kinematic stimulus variable that crosses the zero correlation level within the time window expected for a functional delay. Because our stimuli are characterized by l/v but also by $θ_0$, we checked whether, for 140 ms delay, the angular increment also showed a zero correlation coefficient with $θ_0$. The analysis revealed that in fact, with 140 ms delay, the correlation value is not significantly different from zero (ρ=–0.10±0.14, 95% confidence intervals estimated using the bootstrap method) (Wasserman, 2004).

The two different methods of analysis described above led us to the same conclusion: crabs make the decision to initiate the escape when the stimulus angular increment reaches 7 deg (Fig. 5F).

The escape run is under continuous visual regulation

In many animals, the escape behavior to predator attacks often represents a ballistic movement [e.g. the crayfish tailflip (Liden and Herberholz, 2008) and the C-start escape response of fish (Preuss et al., 2006)]. Thus, once the response has been launched, it goes to completion without adjustments related to changes in the eliciting stimulus. This does not seem to be the case for the crab's escape run. To investigate the dependency of the escape response on the incoming visual information, we performed an experiment using the same looming stimulus, but we stopped it at different stages of its growth. Fig. 7 shows that immediately after the stimulus finished growing, the escape run always decelerated. The result clearly shows that the escape run is under continuous, rather than ballistic, visual regulation.

An input–output relationship for the regulation of the animal escape speed

The results shown in Fig. 7 indicate that the crab continually senses the stimulus expansion and adjusts the motor output accordingly.
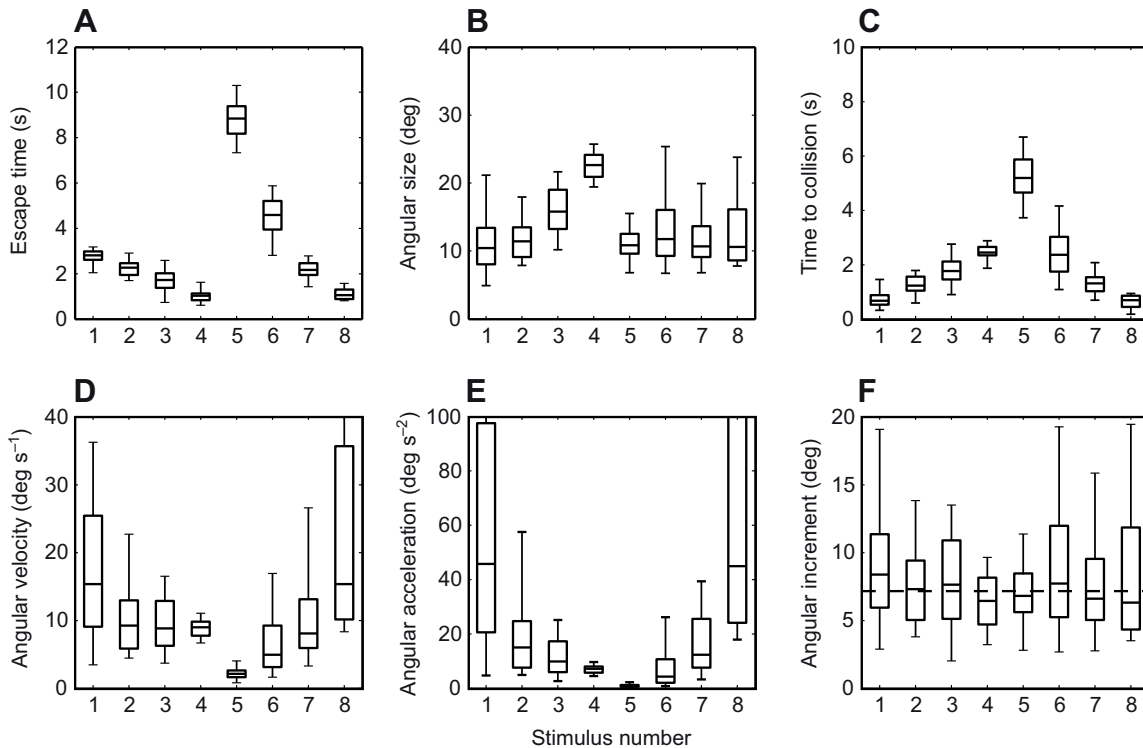
Fig. 5. Stimulus optical variables and the decision to escape. We analyzed whether any of the variables Z_{1-6} ($t_{esc}-\delta$) described in Table 2 attained a constant value with all the stimuli when animals decided to initiate the escape run. Out of the six variables analyzed, angular increment was the only one whose value remained constant throughout the different stimuli ($P=0.6$). On average, crabs made the decision to escape when the apparent size of the stimulus increased beyond 7 ± 0.3 deg (mean ± s.e.m.; dashed line in F).

Moreover, a cursory inspection of Fig. 2 suggests that the escape speed of the animals is related to the dynamics of the stimulus expansion. In fact, those stimuli presenting the fastest expansion dynamics (corresponding to the smaller or the faster approaching objects of the series) exhibited the steepest gain of escape speed, whereas those presenting the slower expansion rate (corresponding to the larger or slower approaching objects) resulted in more gradual speed changes. Therefore, it is quite apparent that crabs adjust their speed as a function of the image expansion rate. We then attempted to find a phenomenological input–output relationship (f_{IO}) that depended only on one of the optical variables of the looming stimuli $Z_{1-6}(t)$ to describe the animal's escape response. Ideally, this function should be able to describe the condition when animals are still [$v_c(t)=0$], as well as the changes in speed after escape initiation. The relationship between the speed of the crab v_c, the optical variable Z, and the input–output relationship is given by: $v_c(t)=f_{IO}[Z(t-\delta)]$. A description of this type implies searching for different potential optical variables and f_{IO} functions. Among the optical variables described in Table 2, the only one that could describe the entire escape response (both the initiation and the speed of the escape run) is $\Delta\theta$ (remember that the escape run starts invariably when $\Delta\theta$ reaches a threshold value of $\Delta\theta_{esc}=7$ deg). Therefore, we incorporated $\Delta\theta$ into our description, as it is the optical variable that best predicts whether the animal is at rest or escaping. Our first approach was to extend the prediction on escape initiation to escape speed by using $\Delta\theta$ only. To write this hypothesis mathematically, we defined the variable $u_1(t-\delta)=\Delta\theta(t-\delta)-\Delta\theta_{esc}$ to fulfil the following: if $\Delta\theta<\Delta\theta_{esc}$, then u_1 is negative and the animal remains still; if $\Delta\theta\geq\Delta\theta_{esc}$, then u_1 is positive and the animals escape with speed $v_c(t)>0$.

In Fig. 8 we illustrate our analysis using a hypothetical case. Fig. 8A shows the angular increment $\Delta\theta$ as a function of time and Fig. 8B shows the variable $u_1(t-\delta)$. The variable u_1 is obtained by subtracting from the variable $\Delta\theta$ a fixed $\Delta\theta_{esc}$ value (note the difference in the y-axis scale). This determines two regions separated by the black horizontal dashed line: for values of u_1 below the line the animal would decide to remain motionless (exemplified by the blue circle), when u_1 intercepts the line the animal would decide to initiate the escape (green circle), and for values of u_1 above the line the animal would be escaping (red circle). Once u_1 has been defined, we need to propose a possible function f_{IO} to describe the speed of the animals. For this, it is important to take into account the fact that animals operate with motor and sensory processes that have saturation limits (Blickham and Full, 1987; Gabbiani et al., 1999). These limits constrain the performance of the animal and hence must be considered in a description of the escape speed. We propose:

$$v_c = f_{IO}(u_1) = v_{1,max} \cdot \frac{u_1}{u_{1,50\%} + u_1} \quad \text{if} \quad u_1 \geq 0 , \tag{6}$$

$$v_c = f_{IO}(u_1) = 0 \quad \text{if} \quad u_1 < 0 . \tag{7}$$

This saturating function is described by the parameters $v_{1,max}$ and $u_{1,50\%}$. The parameter $v_{1,max}$ corresponds to the maximum speed the animal can reach and the parameter $u_{1,50\%}$ is the value of the variable u_1 when the animal reaches 50% of $v_{1,max}$. Fig. 8C shows the function f_{IO} and the geometric representation of $v_{1,max}$ and $u_{1,50\%}$. Another important parameter used to characterize f_{IO} is its slope at $u_1=0$. The slope, called m_1, depends on $v_{1,max}$ and $u_{1,50\%}$ as follows: $m_1=v_{1,max}/u_{1,50\%}$ (Fig. 8C). m_1 will be used later to compare responses
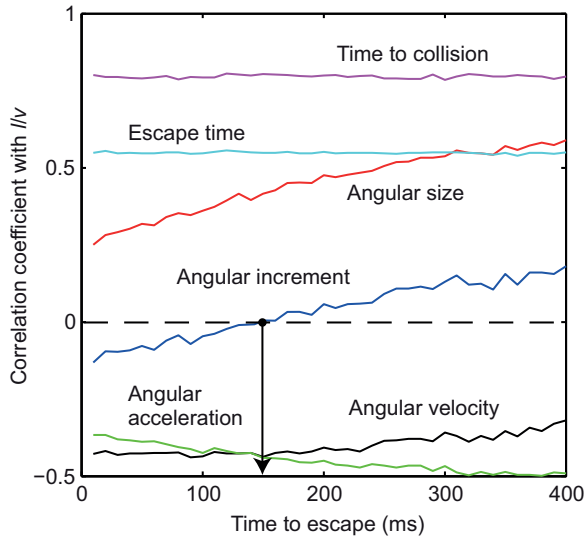
Fig. 6. Correlation between stimulus l/v and five kinematic variables as a function of time. Twenty crabs were presented with the eight looming stimuli with different l/v values reported in Table 1 (one trial per stimulus and per crab). Correlations between l/v and instantaneous angular size, increment, velocity, acceleration and time to collision were computed in 10 ms steps. The only kinematic stimulus variable that crosses the zero correlation level within the time window expected for a functional delay is angular increment. See Results for details.
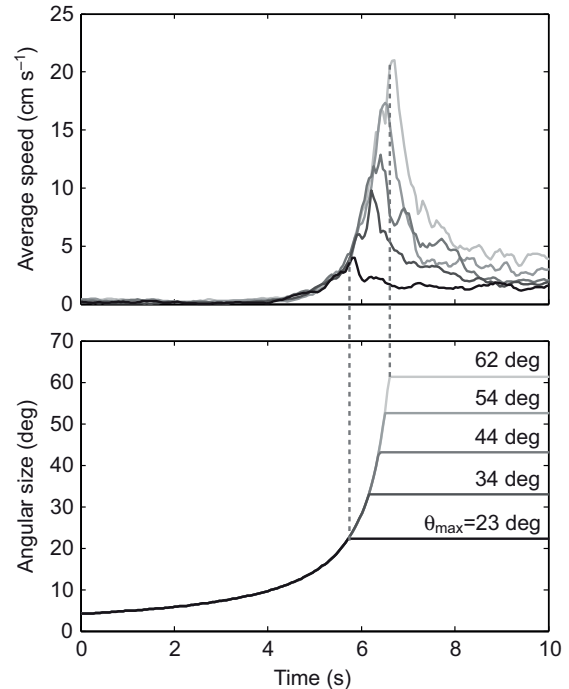

Fig. 7. The escape run is under continuous visual regulation. To investigate the dependency of the escape speed on the incoming visual information, we performed an experiment using the same looming dynamics (l=17 cm, v=71.5 cm s^{-1}), but stopping its expansion at different angular sizes (θ_{max}=23, 34, 44, 54 and 62 deg). Traces show average speed of animals in response to the five stimuli shown below. Note that immediately after the stimulus stopped growing, the escape run always decelerated. Each stimulus was applied twice to each animal (N=6 animals).

with the different stimuli. Fig. 8, then, shows step by step how we obtained a prediction of the animal's speed $v_c(t)$ using the function f_{IO}. (1) We started with a stimulus value of $\Delta\theta$ (Fig. 8A). (2) We then calculated $u_1(t-\delta)=\Delta\theta(t-\delta)-\Delta\theta_{esc}$ (Fig. 8B). (3) We introduced the value of $u_1(t-\delta)$ in f_{IO} (black dashed arrow from Fig. 8B to 8C) to calculate the crab's speed $v_c(t)=f_{IO}[u_1(t-\delta)]$ (vertical arrows in Fig. 8C). (4) Finally, we obtained the speed predicted by f_{IO} as a function of time (horizontal arrows from Fig. 8C to D).

Fig. 9A shows examples of speed fits using the f_{IO} of Eqns 6 and 7 for the eight stimuli in a single crab. We fitted individual records (N=20 animals, eight stimuli per animal) for the time interval ranging from t_{esc} to the end of the expansion. For each record, we determined t_{esc} as explained in the Materials and methods. Then we obtained $\Delta\theta_{esc}$ and u_1. Finally, we determined f_{IO} parameters ($v_{1,max}$, $u_{1,50\%}$ and m_1) by least-square fits in each record. After obtaining the f_{IO} parameters for all trials, we tested whether each of these values was the same or whether they differed among the different stimuli (Fotowat and Gabbiani, 2007). As for escape initiation, common values mean that with the proposed f_{IO}, using u_1 alone, we could predict the speed of each crab independent of the stimulus applied. However, Fig. 9B–D shows that the values of $v_{1,max}$, $u_{1,50\%}$ and m_1 are significantly different among stimuli ($P\leq0.01$ for the three parameters). Therefore, the proposed function failed to describe the escape response.

An inspection of Fig. 9D reveals that m_1 is highest for stimuli with the fastest expansion dynamics (stimuli 1 and 8). This suggests that the angular velocity of the stimulus affects the speed of the escape response. In fact, angular velocity $\dot{\theta}(t)$ is an optical variable central to those models describing the response of looming sensitive neurons in different animal species [e.g. locusts (Hatsopoulos et al., 1995; Gabbiani et al., 2002) and pigeons (Sun and Frost, 1998)]. The simplest operation available to include angular velocity in our description of the crab's escape response would be to add it to the stimulus angular increment in the form $u_2(t)=u_1(t)+\beta\dot{\theta}(t)$, where β

is a proportionality constant. But, because $\dot{\theta}(t)$ has a positive value from the very beginning of the stimulus approach, this $u_2(t)$ does not satisfy the requirement of crossing the zero value when the decision to escape is made (see Fig. 5D).

Another way of including the stimulus' angular velocity would be as a multiplicative factor. In fact, a multiplicative computation proved to be performed by visual neurons sensitive to looming (Gabbiani et al., 2002). We then propose a new variable $u_2(t)$ that incorporates the angular velocity $\dot{\theta}(t)$ as a product:

$$u_2(t) = u_1(t)\,\dot{\theta}(t) = [\Delta\theta(t) - \Delta\theta_{esc}]\,\dot{\theta}(t). \qquad (8)$$

This proposal is justified because: (1) $u_2(t_{esc}-\delta)=0$ when the escape initiates, because $u_1(t_{esc}-\delta)=0$, as shown before; and (2) the product of $u_1(t)$ and $\dot{\theta}(t)$ results in a greater reduction of m_1 for those stimuli with the fastest expansion dynamics, which helps cancel out the differences in the slopes obtained with the former variable $u_1(t)$ (Fig. 9D, stimuli 1 and 8).

Fig. 10A shows examples of speed fits using the f_{IO} with variable u_2 of Eqn 8 for the eight stimuli in a single crab. Following the procedure described above, but now using Eqn 8, we obtained $v_{2,max}$, $u_{2,50\%}$ and m_2 in every trial and evaluated their independence. Fig. 10B–D shows that, using the variable $u_2(t)$, the parameters $v_{2,max}$, $u_{2,50\%}$ and m_2 do not differ significantly among the stimuli ($v_{2,max}$: P=0.4; $u_{2,50\%}$: P=0.7; m_2: P=0.5). These results suggest that we have found a phenomenological input–output relationship entailing the product of the stimulus angular increment $\Delta\theta$ and the angular velocity $\dot{\theta}$, which successfully predicts the escape performance upon a wide variety of looming stimuli.
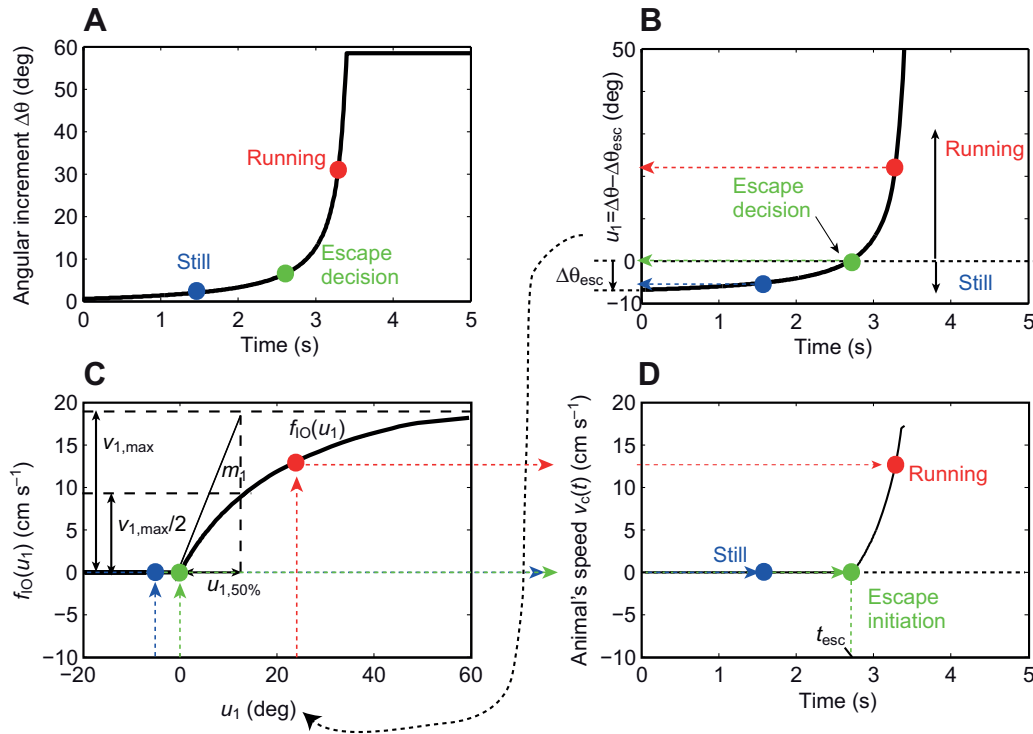
Fig. 8. Illustration of the escape response model using a phenomenological input–output relationship f_{IO}. To attempt to characterize the escape response within each trial, we used a model described by the input–output relationship given by $v_c(t)=f_{IO}[u_1(t-\delta)]$. (A) Stimulus angular increment $\Delta\theta$ as a function of time. (B) Input optical variable $u_1(t-\delta)=\Delta\theta(t-\delta)-\Delta\theta_{esc}$ as a function of time. This variable allowed us to determine whether the animal was still ($u_1<0$, blue circle), the time of the escape decision ($u_1=0$, green circle) or whether the animal was escaping ($u_1>0$, red circle). (C) The variable u_1 was inserted in the input–output relationship f_{IO}, which provided the predicted animal's speed v_c. Note that f_{IO} depends on the value of $\Delta\theta_{esc}$, $v_{1,max}$ and $u_{1,50\%}$. Besides, f_{IO} is also characterized by its slope at $u_1=0$. The slope, called m_1, depends on $v_{1,max}$ and $u_{1,50\%}$ as follows: $m_1=v_{1,max}/u_{1,50}$. (D) Prediction of the animal's speed as a function of time using the f_{IO} model. See Results for further explanations.

The following equations summarize our visuo-motor transformation model of the crab's escape performance.

$$u_2(t) = u_1(t)\cdot\dot\theta(t) = [\Delta\theta(t) - \Delta\theta_{esc}]\cdot\dot\theta(t) , \quad (9)$$

$$v_c(t) = f_{IO}\left[u_2(t-\delta)\right]$$

$$= v_{2,max}\cdot\frac{u_2(t-\delta)}{u_{2,50\%} + u_2(t-\delta)} \quad \text{if} \quad u_2(t-\delta)\geq 0 , \quad (10)$$

$$v_c(t) = 0 \quad \text{if} \quad u_2(t-\delta)<0 . \quad (11)$$

Fig. 11 shows the animals' speed as predicted by Eqns 9–11, superimposed against the mean speed of the group of crabs ($N=20$) of Fig. 2. The prediction was made by estimating the values of $\Delta\theta_{esc}$, $v_{2,max}$ and $u_{2,50\%}$ as follows: $\Delta\theta_{esc}=7$ deg was the mean value obtained in Fig. 5F, whereas $v_{2,max}=17$ cm s^{-1}, $u_{2,50\%}=490$ deg^2 s^{-1} and $m_2=0.035$ cm deg^{-2} were the mean values obtained in Fig. 10B–D. The good matching between the predicted and the actual mean speed of crabs for all the stimuli tested indicates that the fits generated with these optical values are largely satisfactory.

DISCUSSION

The relevance of studying the mechanisms by which animals detect approaching objects and avoid collisions is well recognized (for reviews, see Rind and Simmons, 1999; Fotowat and Gabbiani, 2011). Studies in pigeons have revealed that specialized visual neurons carry out several different computations in parallel to analyze signals from approaching objects such as predators (Sun and Frost, 1998),

indicating that information used to avoid collisions can be obtained in different ways (Laurent and Gabbiani, 1998). In addition, the motor network and muscular machinery for generating escape behavior in animals such as pigeons, fish, locusts or crabs are largely different. Thus, comparative studies have been called for to understand how sensory-motor integration contributes to decision-making in the context of collision-avoidance behaviors and learn whether common sensory-motor transformation rules are exploited by different species (Fotowat and Gabbiani, 2011).

In a previous study, we introduced the crab as a new model with which to study collision-avoidance behaviors. We have shown that the behavior of crabs upon the sight of a predator attack happening in the wild can be reliably elicited and thoroughly measured in the laboratory using 2-D computer simulations and a treadmill-like device. We also showed that identified neurons of the lobula (similar to those studied in the locust), which seem to play a central role in this behavior, can be recorded in the living animal (Oliva et al., 2007). Therefore, crabs emerge as an attractive model that we can use to contribute to our understanding of the processes involved in collision-avoidance behaviors.

In the present study we performed a systematic behavioral analysis of responses to a wide variety of looming stimuli to identify which parameters are used by the crab to initiate an escape run, and determine its speed. The main findings can be summarized as follows: (1) the decision to initiate the escape response is made on fixed criteria, i.e. when the angular size increases by 7 deg (Fig. 5F); (2) the escape run is not a ballistic all-or-none type of response,
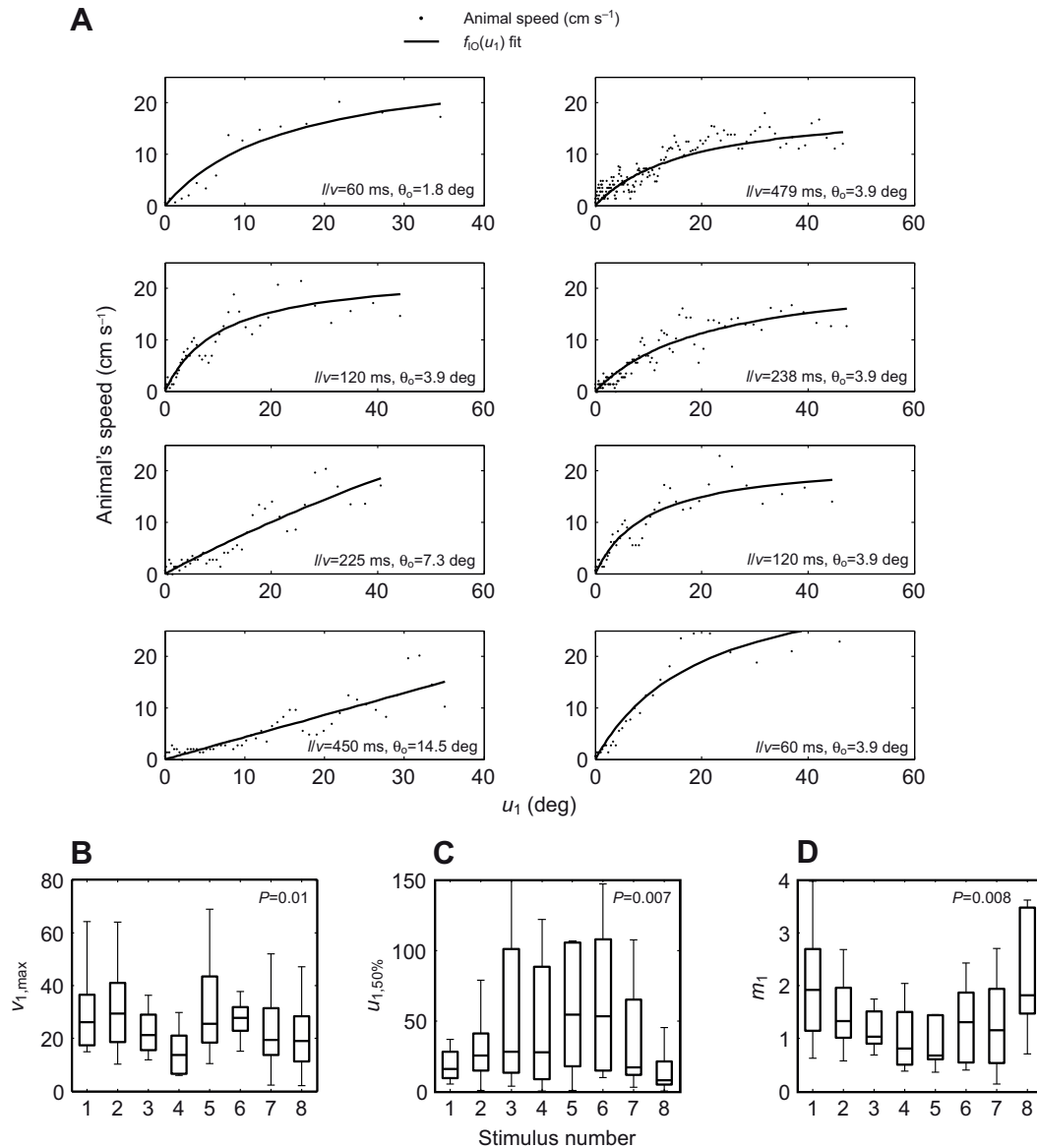
A

B **C** **D**

Fig. 9. (A) Example of escape response fits using the input–output relationship $v_c = f_{IO}[u_1]$ for the eight stimuli in a single crab. Fits were made for the time interval ranging from t_{esc} to the end of the expansion. For each record t_{esc} was determined as explained in the Materials and methods, then we obtained $\Delta\theta_{esc}$ and, finally, $u_1(t-\delta) = \Delta\theta(t-\delta) - \Delta\theta_{esc}$ was calculated. The parameters of f_{IO} ($v_{1,max}$, $u_{1,50\%}$) were determined by least-square regression for each record using Eqns 6 and 7. Left and right columns show fits of responses to stimuli 1–4 and 5–8 of Table 1, respectively. Responses were individually fitted for all the animals (N=20 animals, eight stimuli per animal). (B–D) Values of $v_{1,max}$, $u_{1,50\%}$ and m_1 obtained after fitting the input–output relationship $v_c = f_{IO}[u_1]$ for all trials. After obtaining f_{IO} using u_1 (Eqns 6 and 7), we tested whether $v_{1,max}$, $u_{1,50\%}$ and m_1 remained constant throughout the stimuli. As shown in B–D, the analyses revealed significant differences for the three parameters.

because its speed is adjusted concurrently with changes in the stimulus optical variables (Figs 2, 7); and (3) the escape performance can be faithfully predicted (Fig. 11) by a phenomenological input–output relationship depending on a multiplicative operation of the stimulus angular increment and angular velocity (Eqns 9–11).

The decision to initiate the escape run

A central issue regarding avoidance responses to approaching objects is knowing which one of the various optical parameters of the expanding image is used by the animal to decide when to start the response. In agreement with our present results in *N. granulata*, studies in other crustaceans have shown that the decision is made based on an increase in the apparent size of the stimulus. For

instance, the critical stimulus parameter to initiate the escape run in the crab *Heloecius* was found to be an increase of 5.6 deg (see Hemmi, 2005b), whereas in the crayfish the required increase was ~8 deg (Glantz, 1974). In a previous study using a single looming stimulus, we reported that *N.* (=*Chasmagnathus*) *granulata* started the escape when the angular size of the stimulus had grown by approximately 10 deg (Oliva et al., 2007), which is 3 deg above the angular increment reported here. This discrepancy comes from the fact that in our previous study we did not take into account the delay time between the visual stimulus and the response recording, as was considered in the present study (Fig. 3). The present value of $\Delta\theta_{esc} = 7$ deg is in perfect agreement with those reported for *Heloecius* and crayfish.
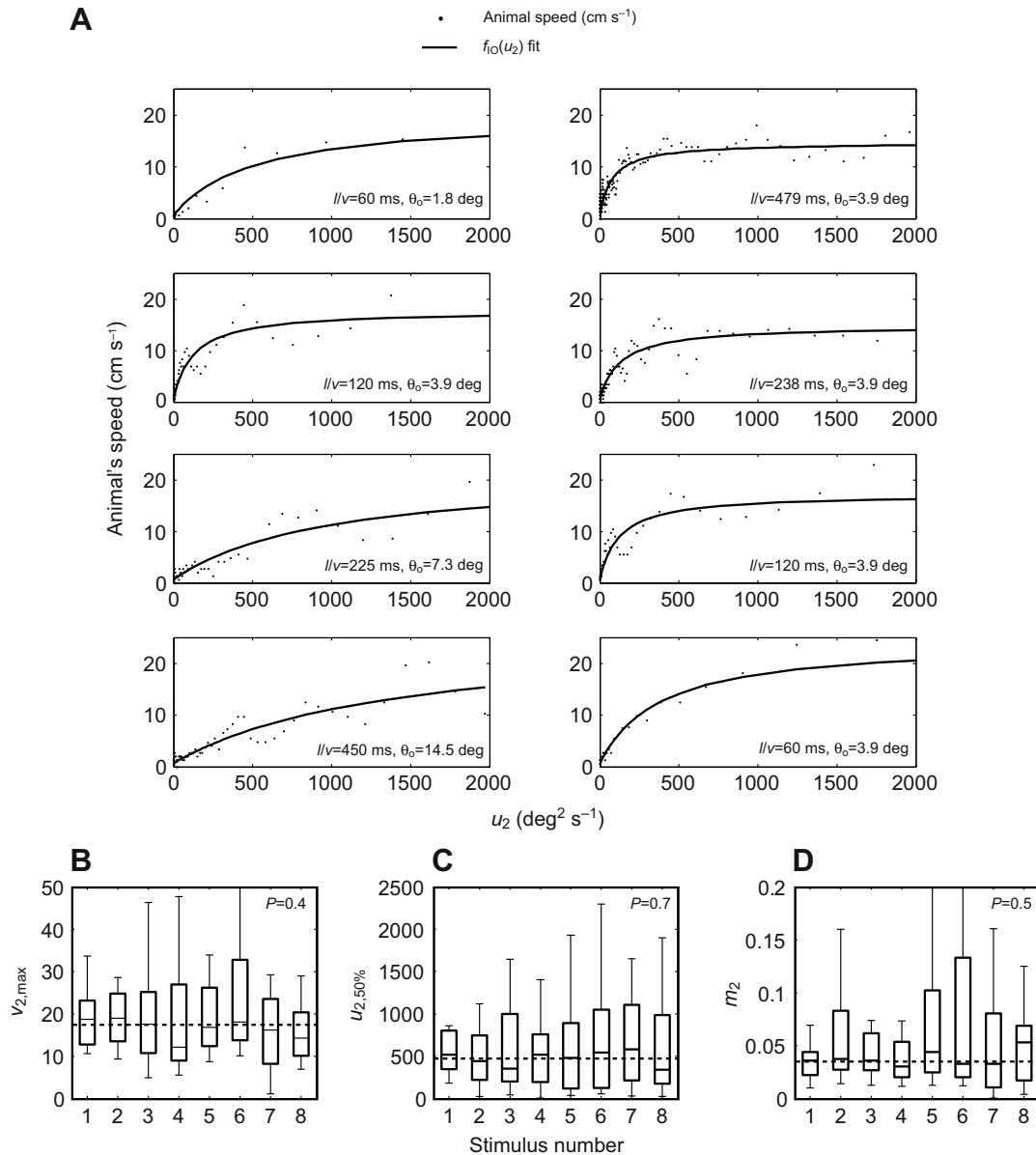
A

B

C

D

Fig. 10. (A) Example of escape response fits using the input–output relationship $v_c = f_{IO}[u_2]$ for the eight stimuli in a single crab. Fits were made for the time interval ranging from t_{esc} to the end of the expansion. For each record, t_{esc} was determined as explained in the Materials and methods, then we obtained $\Delta\theta_{esc}$ and, finally, $u_2(t-\delta)$ was calculated. The parameters of f_{IO} ($v_{2,max}$, $u_{2,50\%}$) were determined by least-square regression for each record using Eqn 8. Left and right panels show fits of responses to stimuli 1–4 and 5–8 of Table 1, respectively. Responses were individually fitted for all the animals (N=20 animals, eight stimuli per animal). (B–D) Values for $v_{2,max}$, $u_{2,50\%}$ and m_2 obtained by fitting the input–output relationship $v_c = f_{IO}[u_2]$ for all trials. After obtaining f_{IO} using u_2 (Eqn 8), we tested whether $v_{2,max}$, $u_{2,50\%}$ and m_2 remained constant throughout the stimuli. As shown in B–D, the analyses did not reveal significant differences for any of the three parameters.

However, studies with fiddler crabs performed in the field by Hemmi and Pfeil depicted a different scenario (Hemmi, 2005a; Hemmi, 2005b; Hemmi and Pfeil, 2010). These studies showed that the escape response to an approaching dummy predator includes different stages, each of which would be triggered by a different parameter of the visual stimulus. For instance, retinal speed may lead to an initial freeze followed by a run towards the burrow entrance, where the crab may stay and assess whether there is an increase in the stimulus' apparent size before deciding to descend into the burrow. The progression along these different response stages has been related to an escalation of the predation risk imposed by the stimulus closeness (Hemmi, 2005a). These field studies in fiddler crab were carried out using a dummy that always approached the crabs with variable deviations away from the collision course. Such stimuli would present a lower risk than a similar stimulus that approaches the crab directly. Surprisingly, however, the indirect stimulus elicited earlier responses than the direct one. This is because, at a long distance, an object moving tangential to the crab generates greater retinal motion than a pure looming stimulus, which can be used by the animal to perform an earlier kind of startle response [for a discussion of this apparent paradox, see Hemmi (Hemmi, 2005a; Hemmi, 2005b)]. In contrast with these field studies, our laboratory experiments enabled us to disentangle the looming stimulus from any translational motion
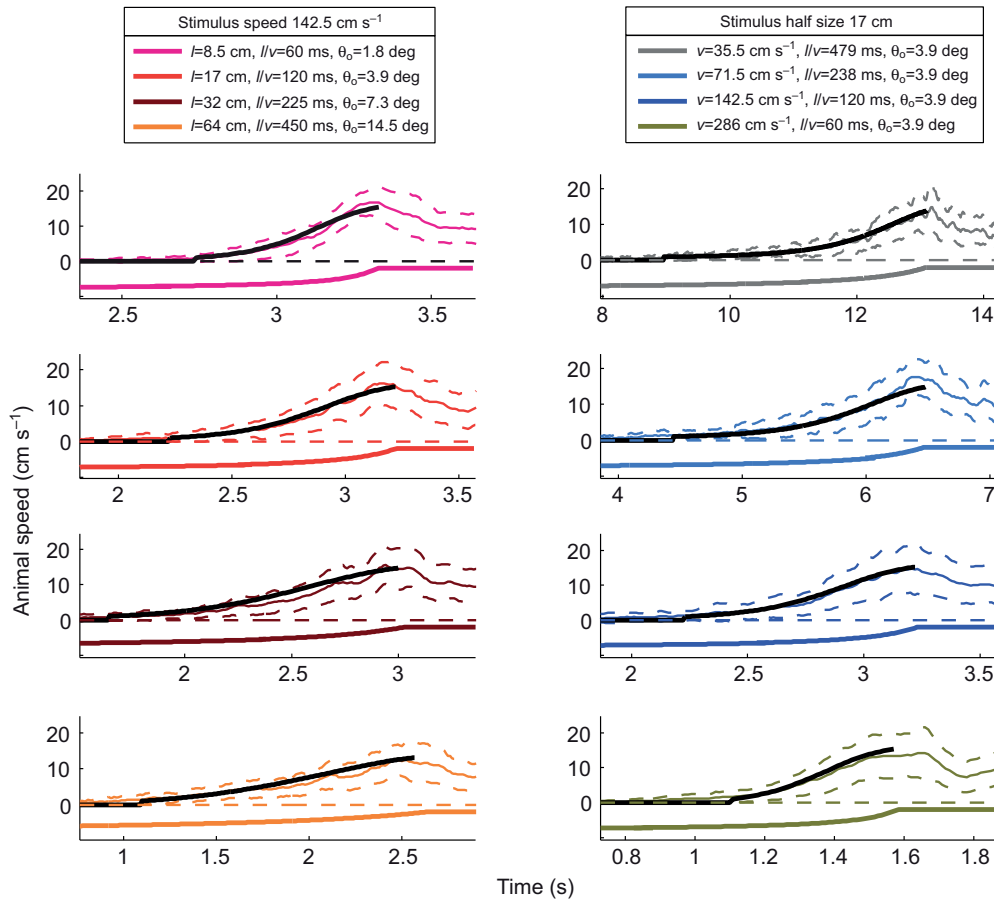
Fig. 11. Mean speed and predicted speed responses for all the tested stimuli (left column: stimuli 1–4; right column: stimuli 5–8) using the input–output relationship $v_c=f_{IO}[u_2]$ (Eqns 9–11). The curves illustrate the segment of data corresponding to the time of stimulus expansion (dashed line rectangles in Fig. 2). Black traces indicate the predicted speed. The predicted values were obtained by using the proposed input–output relationship $v_c=f_{IO}[u_2]$, with mean parameter values estimated from experimental data ($\Delta\theta_{esc}$=7 deg, $v_{2,max}$=17 cm s^{-1} and $u_{2,50\%}$=490 deg^2 s^{-1}).

component, and thus investigate the computations underlying the detection of visual stimuli approaching on a direct collision course with the animal.

Regulation of the escape speed

In crabs, the escape behavior in response to visual stimuli is far from a simple reflex, but rather a finely tuned, complex behavioral sequence that is modulated at all levels of organization (for a review, see Hemmi and Tomsic, 2012). Therefore, our finding that crabs continuously adjust their escape speed according to ongoing information provided by the visual stimulus (Figs 2, 7) is not surprising. However, the possibility of measuring the changes in the speed of the escape run and relating them to concurrent changes in the stimulus optical parameters offers a remarkable opportunity for studying the visuo-motor transformation underlying a non-ballistic kind of behavior.

Early studies of Wiersma and collaborators on crustaceans revealed the existence of neurons sensitive to different types of visual motion (reviewed in Wiersma et al., 1982). More recently, we identified a few classes of lobula giant (LG) neurons that are highly sensitive to looming stimuli (Medan et al., 2007; Oliva et al., 2007). Moreover, we showed that the firing rate of these neurons increases with the stimulus angular expansion in a way that appears to anticipate the animal's speed of run [fig. 9 in Oliva et al. (Oliva et al., 2007)]. That study, however, was performed using a single looming stimulus, which precluded making quantitative analyses relating the stimulus' expansion dynamics to the LG neurons' firing rates, and relating these with the animals' speed. The results presented here will make it possible to investigate these relationships. We are currently recording the response of the LGs to the full set

of looming stimuli used in the present study. Our preliminary results indicate that the LGs may indeed play a central role in the visuo-motor transformations occurring during the escape response to approaching objects in the crab.

Behavioral studies in simplified laboratory conditions and the complexity of the real world

An animal behaving in its natural environment has to relentlessly make behavioral decisions based on the flow of incoming information and its previous experience. Although at first sight the crab's avoidance response to an approaching predator may appear as a simple reflex behavior, this is clearly not the case. Upon detection of the approaching stimulus, crabs, like many animals, have to decide whether, when, in which direction and how intensely to perform an escape response. Each one of these decisions is known to be strongly affected by environmental and behavioral contexts, such as the animal's position relative to a refuge, and by the animal's learnt experiences (Hemmi and Tomsic, 2012). But if the environment is so important in shaping the avoidance behavior, what can we learn about the results from studies performed in simplified and rather artificial laboratory conditions? The answer is straightforward. As long as the essence of the behavior is preserved, we can use the well-controlled stimulation conditions to investigate the fundamental features of the response. Characterizing the response to simple stimuli is a requisite for identifying neurons important for such behavior, and for understanding the way these neurons perform their fundamental operations.

FUNDING

REFERENCES

Berón de Astrada, M. and Tomsic, D. (2002). Physiology and morphology of visual movement detector neurons in a crab (Decapoda: Brachyura). *J. Comp. Physiol. A* **188**, 539-551.

Berón de Astrada, M. B., Bengochea, M., Medan, V. and Tomsic, D. (2012). Regionalization in the eye of the grapsid crab *Neohelice granulata* (=*Chasmagnathus granulatus*): variation of resolution and facet diameters. *J. Comp. Physiol. A* **198**, 173-180.

Blickham, R. and Full, R. J. (1987). Locomotion energetics of the ghost crab. II. Mechanics of the center of mass. *J. Exp. Biol.* **130**, 155-174.

Borst, A. and Bahde, S. (1988). Spatio-temporal integration of motion – a simple strategy of safe landing in flies. *Naturwissenschaften* **75**, 265-267.

Card, G. and Dickinson, M. H. (2008a). Visually mediated motor planning in the escape response of *Drosophila. Curr. Biol.* **18**, 1300-1307.

Card, G. and Dickinson, M. (2008b). Performance trade-offs in the flight initiation of *Drosophila. J. Exp. Biol.* **211**, 341-353.

Fotowat, H. and Gabbiani, F. (2007). Relationship between the phases of sensory and motor activity during a looming-evoked multistage escape behavior. *J. Neurosci.* **27**, 10047-10059.

Fotowat, H. and Gabbiani, F. (2011). Collision detection as a model for sensory-motor integration. *Annu. Rev. Neurosci.* **34**, 1-19.

Fotowat, H., Harrison, R. R. and Gabbiani, F. (2011). Multiplexing of motor information in the discharge of a collision detecting neuron during escape behaviors. *Neuron* **69**, 147-158.

Fry, S. N., Rohrseitz, N., Straw, A. D. and Dickinson, M. H. (2009). Visual control of flight speed in *Drosophila melanogaster. J. Exp. Biol.* **212**, 1120-1130.

Gabbiani, F., Krapp, H. G. and Laurent, G. (1999). Computation of object approach by a wide-field, motion-sensitive neuron. *J. Neurosci.* **19**, 1122-1141.

Gabbiani, F., Krapp, H. G., Koch, C. and Laurent, G. (2002). Multiplicative computation in a visual neuron sensitive to looming. *Nature* **420**, 320-324.

Glantz, R. M. (1974). Defense reflex and motion detector responsiveness to approaching targets: the motion detector trigger to the defense reflex pathway. *J. Comp. Physiol.* **95**, 297.

Gray, J. R., Lee, J. K. and Robertson, R. M. (2001). Activity of descending contralateral movement detector neurons and collision avoidance behaviour in response to head-on visual stimuli in locust. *J. Comp. Physiol. A* **187**, 115-129.

Hatsopoulos, N., Gabbiani, F. and Laurent, G. (1995). Elementary computation of object approach by wide-field visual neuron. *Science* **270**, 1000-1003.

Hemmi, J. M. (2005a). Predator avoidance in fiddler crabs: 1. Escape decisions in relation to the risk of predation. *Anim. Behav.* **69**, 603-614.

Hemmi, J. M. (2005b). Predatory avoidance in fiddler crab: 2. The visual cues. *Anim. Behav.* **69**, 615-625.

Hemmi, J. M. and Pfeil, A. (2010). A multi-stage anti-predator response increases information on predation risk. *J. Exp. Biol.* **213**, 1484-1489.

Hemmi, J. M. and Tomsic, D. (2012). The neuroethology of escape in crabs: from sensory ecology to neurons and back. *Curr. Opin. Neurobiol.* **22**, 194-200.

Land, M. and Layne, J. E. (1995). The visual control of behaviour in fiddler crabs. II. Tracking control systems in courtship and defence. *J. Comp. Physiol. A* **177**, 91.

Laurent, G. and Gabbiani, F. (1998). Collision-avoidance: nature's many solutions. *Nat. Neurosci.* **1**, 261-263.

Liden, W. H. and Herberholz, J. (2008). Behavioral and neural responses of juvenile crayfish to moving shadows. *J. Exp. Biol.* **211**, 1355-1361.

Medan, V., Oliva, D. and Tomsic, D. (2007). Characterization of lobula giant neurons responsive to visual stimuli that elicit escape behaviors in the crab *Chasmagnathus. J. Neurophysiol.* **98**, 2414-2428.

Oliva, D. (2010). Mechanisms of visual detection and avoidance of collision stimuli in a new experimental model: the crab *Chasmagnathus granulatus*. PhD thesis, University of Buenos Aires, Argentina.

Oliva, D., Medan, V. and Tomsic, D. (2007). Escape behavior and neuronal responses to looming stimuli in the crab *Chasmagnathus granulatus* (Decapoda: Grapsidae). *J. Exp. Biol.* **210**, 865-880.

Preuss, T., Osei-Bonsu, P. E., Weiss, S. A., Wang, C. and Faber, D. S. (2006). Neural representation of object approach in a decision-making motor circuit. *J. Neurosci.* **26**, 3454-3464.

Rind, F. C. and Simmons, P. J. (1999). Seeing what is coming: building collision-sensitive neurones. *Trends Neurosci.* **22**, 215-220.

Santer, R. D., Simmons, P. J. and Rind, F. C. (2005a). Gliding behaviour elicited by lateral looming stimuli in flying locusts. *J. Comp. Physiol. A* **191**, 61-73.

Santer, R. D., Yamawaki, Y., Rind, F. C. and Simmons, P. J. (2005b). Motor activity and trajectory control during escape jumping in the locust *Locusta migratoria. J. Comp. Physiol. A* **191**, 965-975.

Santer, R. D., Rind, F. C., Stafford, R. and Simmons, P. J. (2006). Role of an identified looming-sensitive neuron in triggering a flying locust's escape. *J. Neurophysiol.* **95**, 3391-3400.

Santer, R. D., Yamawaki, Y., Rind, F. C. and Simmons, P. J. (2008). Preparing for escape: an examination of the role of the DCMD neuron in locust escape jumps. *J. Comp. Physiol. A* **194**, 69-77.

Srinivasan, M. V., Zhang, S. W., Chahl, J. S., Barth, E. and Venkatesh, S. (2000). How honeybees make grazing landings on flat surfaces. *Biol. Cybern.* **83**, 171-183.

Sun, H. and Frost, B. J. (1998). Computation of different optical variables of looming objects in pigeon nucleus rotundus neurons. *Nat. Neurosci.* **1**, 296-303.

Sztarker, J. and Tomsic, D. (2008). Neuronal correlates of the visually elicited escape response of the crab *Chasmagnathus* upon seasonal variations, stimuli changes and perceptual alterations. *J. Comp. Physiol. A* **194**, 587-596.

Sztarker, J. and Tomsic, D. (2011). Brain modularity in arthropods: individual neurons that support 'what' but not 'where' memories. *J. Neurosci.* **31**, 8175-8180.

Tammero, L. F. and Dickinson, M. H. (2002). Collision-avoidance and landing responses are mediated by separate pathways in the fruit fly, *Drosophila melanogaster. J. Exp. Biol.* **205**, 2785-2798.

Tomsic, D., Berón de Astrada, M. and Sztarker, J. (2003). Identification of individual neurons reflecting short- and long-term visual memory in an arthropod. *J. Neurosci.* **23**, 8539-8546.

Wang, Y. and Frost, B. J. (1992). Time to collision is signalled by neurons in the nucleus rotundus of pigeons. *Nature* **356**, 236-238.

Wasserman, L. (2004). *All of Statistics. A Concise Course in Statistical Inference*. Berlin: Springer.

Wiersma, C. A. G., Roach, J. L. M. and Glantz, R. M. (1982). Neural integration in the optic system. In *The Biology of the Crustacea. Neural Integration and Behavior*, Vol. 4 (ed. D. C. Sandeman and H. L. Atwood), pp. 1-31. New York: Academic Press.